Available online at www.sciencedirect.com
ScienceDirect
ELSEVIER
Palaeogeography, Palaeoclimatology, Palaeoecology 249 (2007) 351–361
PALAEO
www.elsevier.com/locate/palaeo

The Sr and Nd isotopic variations of the Chinese Loess Plateau during the past 7 Ma: Implications for the East Asian winter monsoon and source areas of loess

Yin-Xi Wang [a,b], Jie-Dong Yang [b,c,*], Jun Chen [d], Kai-Jun Zhang [d,e], Wen-Bo Rao [d]

[a] School of Geographic and Oceanographic Sciences, Nanjing University, 210093, China
[b] Center of Modern Analysis, Nanjing University, Nanjing, 210093, China
[c] State Key Laboratory of Mineral Deposit Research, Nanjing University, Nanjing, 210093, China
[d] Department of Earth Sciences, Nanjing University, Nanjing, 210093, China
[e] Guangzhou Institute of Geochemistry, Key Laboratory of Marginal Sea Geology, Chinese Academy of Sciences, Wushan, Guangzhou, 510640, China

Received 11 September 2006; received in revised form 7 February 2007; accepted 15 February 2007

Abstract

$^{143}Nd/^{144}Nd$ and $^{87}Sr/^{86}Sr$ ratios of the acid-insoluble residues of the red clay and overlying loess–paleosols from the Lingtai profile of the Loess Plateau, China, were investigated. The results show that variations of the $^{87}Sr/^{86}Sr$ ratios of the Lingtai profile can be divided into two stages. From ~7 Ma B.P. to 2.5 Ma B.P., the acid-insoluble residues in the Red Clay (RC) Formation, are characterized by higher $^{87}Sr/^{86}Sr$ ratios with an average of 0.7230. From 2.5 Ma B.P. to the present, the acid-insoluble residues in the Wuchen Loess (WL4-WS1), Lishi Loess (L15-S1), Malan Loess (L1) and Holocene Loess (S0) have relatively lower $^{87}Sr/^{86}Sr$ ratios and display an overall descending trend from 0.7223 at ~2.5 Ma B.P. to 0.7182 at the present. Among three possible interpretations for the variations of $^{87}Sr/^{86}Sr$ ratios of acid-insoluble residues of the loess (provenance change, chemical weathering change, or grain-size distribution change), only grain-size distribution change provides a satisfactory interpretation. This implies that the East Asian winter monsoon strength was weak and relatively stable from ~7 Ma B.P. to ~2.5 Ma B.P., but became continuously enhanced from ~2.5 Ma B.P. to the present. All the red clay and the overlying loess-paleosols in the Lingtai profile have generally identical ε_{Nd} (0), implying that the source regions of these Eolian deposits of the Chinese Loess Plateau may be relatively stable and has not changed since 7 Ma B.P.

Keywords: Nd and Sr isotopes; Red clay; Eolian deposits; Chinese Loess Plateau, East Asian monsoon

1. Introduction

The Loess Plateau in northern China contains the thickest Eolian sediments worldwide and thus can serve as one of the best-preserved archives of Pliocene–Pleistocene environmental evolution. The Loess Plateau is mainly comprised of the Red Clay Formation and the overlying loess–paleosol sequence. The red clay, with a

* Corresponding author. Center of Modern Analysis, Nanjing University, Nanjing, 210093, China. Tel.: +86 25 83592703; fax: +86 25 83592704.
E-mail address: jdyang@nju.edu.cn (J.-D. Yang).

0031-0182/$ - see front matter © 2007 Elsevier B.V. All rights reserved.
doi:10.1016/j.palaeo.2007.02.010

thickness of tens of meters to more than 100 m, began to accumulate at ~4 to 7 Ma B.P., based on magnetostratigraphic studies (Liu et al., 1988b; Zheng et al., 1991; Evans et al., 1991; Ding et al., 1998a; Sun et al., 1998; An et al., 2001). Paleomagnetic measurements at different sites on the Loess Plateau showed that the contact between the red clay and the overlying loess–paleosols is around the Matuyama/Gauss magnetic reversal (Heller and Liu, 1982; Liu et al., 1988b; Kukla and An, 1989; Rutter et al., 1990; Zheng et al., 1991; Ding et al., 1992). The entire Red Clay Formation appears to be strongly pedogenically modified, suggesting a relatively warm–wet climate (Ding et al., 2000). The loess–paleosol sequence has been demonstrated to be a continuous deposit, which is dated back to about 2.5 Ma (Heller and Liu, 1982; Liu, 1985), and is generally believed to have been formed by transportation and accumulation of Eolian dusts carried by the East Asian monsoon (Heller and Liu, 1982; Liu, 1985; Kukla and An, 1989; Rutter et al., 1990; Ding et al., 1993).

The East Asian climate is mainly controlled by the summer monsoon (southeasterly winds) and winter monsoon (northwesterly winds). The archives of the East Asian monsoon change are well preserved in the loess profiles of the Loess Plateau (Liu, 1985). Some proxy records have been put forward to indicate variations in the summer monsoon intensity, such as magnetic susceptibility (An et al., 1991a; Heller et al., 1993; Maher et al., 1994; Liu et al., 1995), pollen and snail assemblages (data reported only from the last interglacial age to the present; Sun et al., 1997; Rousseau and Wu, 1997), Rb/Sr ratios (Chen et al., 2000), and ratios of free iron to total iron contents (Ding et al., 2001a). However, very limited indices have been suggested as indicators of the winter monsoon intensity, such as the abundance of the coarse grain-size fraction (An et al., 1991b; Lu and An, 1997) or quartz grains (data reported only from 130,000 a B.P. to the present, Xiao et al., 1995). Therefore, it is significant to present new and reliable proxy indicators for the winter monsoon intensity. In the present study, we suggest a new proxy of the winter monsoon strength, i.e. $^{87}Sr/^{86}Sr$ ratio of the acid-insoluble residue, and inquire into change of the East Asian winter monsoon strength since 7 Ma B.P.

The stability of material source regions of the Loess Plateau is another important problem for the study on

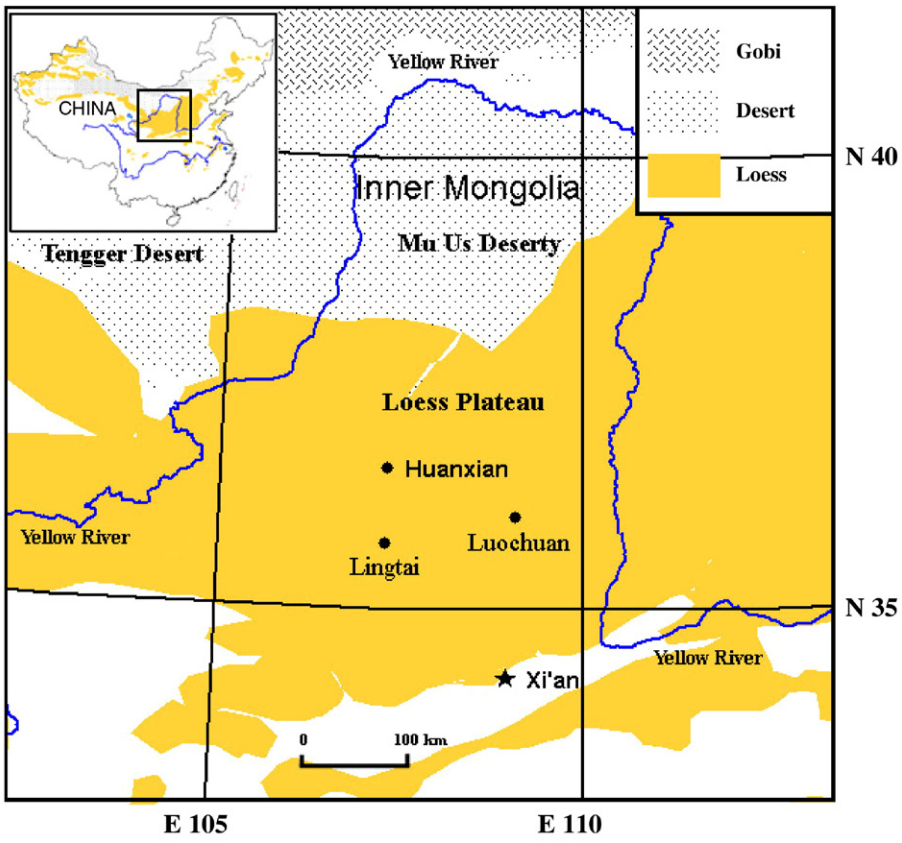

Fig. 1. Sketch map showing the location of the Lingtai profile in the Loess Plateau of China.

the East Asian climate during the Late Cenozoic. At present, many conclusions on the proxy indicators of the East Asian monsoon related to the Loess Plateau are based on the assumption that material source regions of the Loess Plateau have kept no change since 7 Ma B.P.

At present, while numerous Nd and Sr isotopic data for loess and desert samples in different sites in China have been published (for example, Golstein et al., 1984; Nakai et al., 1993; Liu et al., 1994; Jones et al., 1994; Asahara et al., 1995; Honda and Shimizu, 1998; Asahara et al., 1999; Chang et al., 2000; Yokoo et al., 2001; Kanayama et al., 2002; Bory et al., 2003; Yokoo et al., 2004; Nakano et al., 2004), only few investigations (Gallet et al., 1996; Jahn et al., 2001; Sun, 2005) were related to the stability of provenance of loess in a temporally continuous profile of the Loess Plateau. Gallet et al. (1996) and Jahn et al. (2001) investigated Nd and Sr isotopes using bulk soil samples of the Loess Plateau over the past 0.80 Ma to 0.14 Ma, respectively. They concluded that Nd and Sr isotopic compositions of the loess–paleosols are rather uniform and suggest a uniform source region during the period of loess deposition since 0.80 Ma B.P. However, the temporal span (0.80 Ma) investigated by them is too short as compared with 7 Ma of the Loess Plateau. In the present study, we systematically collected the red clays and loess–paleosols in the Lingtai profile and determined the Nd–Sr isotopic compositions of acid-insoluble residues, in an attempt to provide key constraints on the stability of source regions of the Loess Plateau and to reconstruct the East Asian winter monsoon history since 7.0 Ma B.P.

2. The Lingtai profile

The Lingtai profile is located near Lingtai County (35°04′N, 107°33′E), Gansu Province, northern China (Fig. 1). The Lingtai profile consists of a complete loess–soil sequence with a total thickness of 288 m including ≥100 m of the red clay deposits. It comprises a lower unit (Red Clay Formation) and an upper unit (Loess–Paleosol Formation). The Red Clay Formation, unconformably overlies the Mesozoic fluvial–lacustrine sandstones, and could have been deposited from ~7 Ma B.P. to 2.5 Ma B.P. (Liu, 1985; Liu et al., 1988a; Ding et al., 1993). The Loess–Paleosol Formation including the Wuchen Loess (WL4-WS1), the Lishi Loess (L15-S1), the Malan Loess (L1) and the Holocene Loess (S0), has accumulated from 2.5 Ma B.P. to the present (Ding et al., 1998b, 1999). To the best of our knowledge, the Red Clay Formation at Lingtai may contain the thickest red clay sequence in the Loess

Table 1
The determined $^{87}Sr/^{86}Sr$ and $^{143}Nd/^{144}Nd$ ratios of acid-insoluble residues from the Lingtai profile

Horizon	Depth (m)	$^{87}Sr/^{86}Sr$	Depth (m)	$^{143}Nd/^{144}Nd$	$\varepsilon_{Nd}(0)$
L1	5.22	0.718231 (15)	2.30	0.512187 (8)	−8.8
S1	12.30	0.720576 (18)	12.50	0.512184 (9)	−8.9
L2	16.32	0.719126 (16)	16.32	0.512094 (7)	−10.6
S2	20.30	0.720443 (15)	21.10	0.512180 (5)	−8.9
L3	25.12	0.720165 (16)	25.32	0.512172 (8)	−9.1
S3	26.80	0.721098 (16)	26.70	0.512166 (5)	−9.2
L4	30.20	0.720186 (16)	30.40	0.512158 (9)	−9.4
S4	33.70	0.720988 (18)	33.70	0.512105 (9)	−10.4
L5	35.50	0.720123 (17)	35.30	0.512144 (7)	−9.6
S5	42.80	0.721914 (16)	42.70	0.512148 (8)	−9.6
L6	47.40	0.720514 (16)	47.60	0.512155 (6)	−9.4
S6	50.40	0.720858 (16)	50.40	0.512211 (8)	−8.3
L7	54.00	0.721049 (17)	53.80	0.512149 (7)	−9.6
L8			56.00	0.512040 (9)	−9.7
			57.40	0.512178 (8)	−9.0
			57.72	0.512186 (4)	−8.9
S8	58.90	0.720771 (15)	59.10	0.512182 (7)	−8.9
L9	64.52	0.720894 (16)	66.12	0.512177 (9)	−9.0
	66.52	0.720478 (16)			
S9	68.30	0.721152 (19)	68.20	0.512168 (9)	−9.2
L10	71.10	0.721501 (15)	71.10	0.512282 (14)	−6.9
			71.52	0.512157 (3)	−9.4
			71.70	0.512181 (8)	−8.9
S12	75.60	0.721397 (17)	75.90	0.512239 (5)	−9.7
L13	79.40	0.720912 (16)			
S13	81.20	0.721780 (16)	81.50	0.512205 (8)	−8.4
L14	83.00	0.720344 (16)	83.80	0.512183 (9)	−8.9
S14	84.20	0.721298 (16)	84.00	0.512169 (8)	−9.2
L15	87.32	0.720220 (17)	87.50	0.512157 (9)	−9.4
S15	90.80	0.720751 (16)	90.80	0.512141 (7)	−9.7
L16	92.40	0.721102 (17)	92.20	0.512151 (8)	−9.5
S19	101.00	0.721935 (17)	100.00	0.512146 (3)	−9.6
L21	106.00	0.721553 (16)	106.40	0.512167 (6)	−9.2
S22	110.40	0.722354 (16)	110.40	0.512166 (7)	−9.2
L24	118.40	0.721463 (17)	118.60	0.512181 (5)	−8.9
S25	125.60	0.722530 (16)	127.20	0.512174 (7)	−9.1
L26	129.20	0.721909 (17)	129.20	0.512169 (7)	−9.1
S26	131.00	0.722346 (17)	131.60	0.512160 (9)	−9.3
L27	134.00	0.721460 (16)	134.80	0.512142 (6)	−9.6
S27	140.80	0.722744 (16)	140.60	0.512116 (3)	−10.2
L29	144.00	0.721612 (16)	144.00	0.512121 (19)	−10.0
S30	147.80	0.723180 (16)	147.60	0.512124 (9)	−10.0
S31	153.20	0.722222 (15)	153.00	0.512136 (8)	−9.8
	157.00	0.722339 (15)			
	159.40	0.722290 (15)			
L32	161.80	0.722973 (15)	161.80	0.512211 (9)	−8.3
S32	166.60	0.721929 (15)			
L32			154.00	0.512148 (6)	−9.6
			155.00	0.512153 (4)	−9.5
L33	169.60	0.723128 (15)	169.60	0.512152 (8)	−9.5
RC	173.00	0.722963 (16)			
RC	174.80	0.723348 (15)			
RC	187.40	0.723085 (17)			
RC	189.80	0.723262 (15)	189.80	0.512142 (6)	−9.7

(continued on next page)

Table 1 (*continued*)

Horizon	Depth (m)	$^{87}Sr/^{86}Sr$	Depth (m)	$^{143}Nd/^{144}Nd$	$\varepsilon_{Nd}(0)$
RC	193.20	0.722958 (16)			
RC	198.80	0.723418 (17)			
RC	204.00	0.722533 (15)			
RC	210.40	0.722892 (15)			
RC	216.00	0.723414 (16)	216.00	0.512167 (14)	−9.2
RC	222.20	0.722657 (17)			
RC	228.40	0.722951 (15)			
RC	234.60	0.722805 (15)	234.60	0.512119 (6)	−10.1
RC	241.80	0.722196 (16)			
RC	248.80	0.722821 (15)	248.80	0.512147 (8)	−9.6
RC	255.80	0.723532 (17)			
RC	262.60	0.723134 (16)			
RC	269.20	0.722897 (17)	269.20	0.512142 (8)	−9.7
RC	275.20	0.723402 (15)			
RC	280.20	0.723054 (16)			
RC	286.00	0.721931 (16)			
RC			286.40	0.512185 (9)	−8.8

$\varepsilon_{Nd}(0)=[(^{143}Nd/^{144}Nd)_{sample}/(^{143}Nd/^{144}Nd)_{CHUR}-1]\times 10{,}000$, $(^{143}Nd/^{144}Nd)_{CHUR}=0.512638$.
$^{87}Sr/^{86}Sr$ normalized to $^{86}Sr/^{88}Sr=0.1194$, $^{143}Nd/^{144}Nd$ to $^{146}Nd/^{144}Nd=0.7219$.
The numbers in brackets represent error (2σm). RC—red clay, L—loess, S—paleosol.

Plateau. It includes numerous carbonate nodule horizons. A detailed description of the pedostratigraphic units of the Lingtai profile has been given by Ding et al. (1999) and Guo et al. (2004). The red clays are among these nodule levels. They generally contain relatively abundant clay minerals and Fe–Mn minerals, and are likely to have been subjected to strong chemical weathering and pedogenesis (Ding et al., 1998a,b, 1999, 2001a,b).

3. Methods and results

Strontium in the loess and paleosols of the Loess Plateau is found in two groups of minerals. One group is detrital minerals derived from source regions. The other is secondary carbonate, mainly calcite, which formed mostly during pedogenesis (Chen et al., 1997). Therefore, the Sr isotopic composition of the bulk soil sample in the Loess Plateau is affected by pedogenesis and cannot reflect the information on source materials due to the existence of secondary carbonates (Yang et al., 2000, 2001). Therefore, it is necessary first to remove carbonates from the bulk soil sample in order to get rid of influence of pedogenesis. A series of different acid-leaching procedures have been carried out previously by Sheng et al. (2000) and Yang et al. (2001), and the results demonstrated that dilute acetic acid leaching (0.5 M) can dissolve all the calcite in loess samples but does not essentially destroy the structure of detrital minerals (quartz, feldspar, clay minerals and dolomite) derived from source region. The sorting method for the determination of Nd isotopic compositions of the acid-insoluble residue of different grain-size fractions of loess, paleosol and red clay in the Duanjiapo profile of the Loess Plateau, is as follows: first, >45 μm and 45–28 μm fractions were successively obtained by sieving; then, the solution containing the <28 μm fraction was centrifuged (1000 c/m) for 5 min and the residue 28–2 μm fraction. The surviving solution was centrifuged again (5000 c/m) for 30 min and the final residue <2 μm fraction.

$^{87}Sr/^{86}Sr$ ratios of acid-insoluble residues of 63 samples and $^{143}Nd/^{144}Nd$ ratios of acid-insoluble residues of 51 samples in this study were measured (Table 1). The bulk soil samples were gently crushed with a hammer. Grinding was avoided. Carbonates in the sample powders were selectively dissolved with purified 0.5 M acetic acid at room temperature for 4 h. After centrifuging, acid-insoluble residues were digested with an $HNO_3+HF+HClO_4$ mixture and prepared for Sr and Nd isotopic analyses.

Sr and Nd were separated using standard ion exchange techniques (Yang et al., 1997). Sr and Nd isotopic analyses were performed on a VG 354 mass spectrometer with 5 collectors at the Center of Modern Analysis, Nanjing University. Reproducibility and accuracy of Sr isotope runs have been periodically checked by running the Standard Reference Material NBS 987 and Laboratory Standard La Jolla during the past 5 years, with a mean $^{87}Sr/^{86}Sr$ value of 0.710342 ± 0.000040 (certified value: 0.710340 ± 0.000260) and a mean $^{143}Nd/^{144}Nd$ value of 0.511840 ± 0.000008 (uncertainty given as two sigma of the mean), respectively. The analytical blank was <1 ng for Sr and <60 pg for Nd. The $^{87}Sr/^{86}Sr$ and $^{143}Nd/^{144}Nd$ ratios of acid-insoluble residues of the samples from the Lingtai profile are listed in Table 1.

The ages of samples follow Sun and An (2002). The dates of samples are based on the method of Porter and An (1995), that is, the control points are first established according to the dating scales of paleogeomagnetism and then the ages among the control points are determined according to the grain size–age model, as described in detail by Porter and An (1995).

4. Discussion

4.1. Stability of source regions of the Loess Plateau since 7.0 Ma B.P.

The Sr and Nd isotopes of the loess in the Loess Plateau may carry various information, including

Table 2
The $\varepsilon_{Nd}(0)$ values of acid-insoluble residues of four grain-size fractions for the selected three samples (one loess, one paleosol and one red clay) from the Duanjiapo profile

Sample	$^{143}Nd/^{144}Nd$	$\varepsilon_{Nd}(0)$
L1, bulk	0.512186 (4)	−8.8
L1, >45 μm	0.512185 (4)	−8.8
L1, 45–28 μm	0.512200 (9)	−8.5
L1, <28 μm	0.512165 (8)	−9.2
L1, <2 μm	0.512191 (5)	−8.7
S5, bulk	0.512196 (6)	−8.6
S5, >45 μm	0.512200 (6)	−8.5
S5, 45–28 μm	0.512184 (8)	−8.9
S5, <28 μm	0.512175 (9)	−9.1
S5, <2 μm	0.512168 (5)	−9.2
RC, bulk	0.512169 (7)	−9.2
RC, >45 μm	0.512171 (3)	−9.1
RC, 45–28 μm	0.512184 (4)	−8.9
RC, <28 μm	0.512192 (7)	−8.7
RC, <2 μm	0.512199 (5)	−8.5

$^{143}Nd/^{144}Nd$ normalized to $^{146}Nd/^{144}Nd = 0.7219$. RC—red clay, L—loess, S—paleosol.

provenance, monsoon intensity during Eolian transport, chemical weathering and pedogenesis.

Neodymium in the loess of the Loess Plateau exists mainly in detrital minerals derived from source regions and a very small amount of Nd in carbonate. Therefore, after removing the calcite by dilute acetic acid leaching, the Nd isotopic composition of the acid-insoluble residue remains the same as that of the bulk soil sample.

The Nd isotope ratio is generally taken as a powerful tool for source-area identification because minerals and rocks have distinct $^{143}Nd/^{144}Nd$ ratios, depending on their geologic derivation, and the Nd isotope ratio is strongly resistant to alteration in surface chemical weathering and pedogenesis (Golstein et al., 1984; Goldstein and Jacobsen, 1988; Revel et al., 1996; Biscaye et al., 1997; Yokoo et al., 2004; Grousset and Biscaye, 2005).

But no any investigation involving the influence of grain-size sorting, caused by change of monsoon intensity during Eolian transport, on the Nd isotopic ratio of the loess has been reported until now.

Table 2 shows the results determined by us for the Nd isotopic compositions of the acid-insoluble residue of different grain-size fractions of loess, paleosol and red clay in the Duanjiapo profile of the Loess Plateau. The results indicate that the Nd isotopic composition of the acid-insoluble residue, and is only is related to the provenance of the source materials.

Table 1 shows the $\varepsilon_{Nd}(0)$ values in the whole Lingtai profile from 7 Ma B.P. to the present, ranging from −6.9 to −10.6, with an average of −9.3. Except for four anomalous values, the values lie between −8.8 and −9.8. The red clay has a relatively narrow range from to −8.8 to −10.1, with an average of −9.5, and the overlying loess–paleosols have $\varepsilon_{Nd}(0)$ values, ranging from −8.3 to −10.6, with an average of −9.3. The difference between averages of the red clay and overlying loess–paleosols is only 0.2ε units. This indicates the relatively homogeneous $\varepsilon_{Nd}(0)$ values in the whole profile and the provenance of loess of the Lingtai profile is relatively stable and has not changed since 7 Ma B.P.

A recent publication by Sun (2005) described Nd isotopic variations in the Jinchuan profile, only 50 km away from the Lingtai profile, in the Loess Plateau. Although the data of Sun (2005) are similar to ours (Table 3). Sun considered that a change of the source of loess took place and the source of the red clay is different from the overlying loess–paleosols. How much of the fluctuation of $\varepsilon_{Nd}(0)$ in the loess can we recognize as a reliable change of Nd isotopes over time? The answer can be obtained from the determination of analytical error of the isotopic mass spectrometer.

The error of $^{143}Nd/^{144}Nd$ in a single determination in an isotope mass spectrometer is generally within 0.000020, which would lead to a change of $\varepsilon_{Nd}(0)$ within 0.3ε units. In fact, the total experimental error should include the error of $^{143}Nd/^{144}Nd$ for multiple determinations, correction error of Standard Reference Material, and the chemical error of pre-treatment. It is generally accepted to be within ±0.000050, which would lead to a change of $\varepsilon_{Nd}(0)$ within 0.7ε units. Thus, the Nd isotopic composition has changed or an isotopic anomaly takes place only when the difference of $\varepsilon_{Nd}(0)$ between samples is larger than 0.7ε units. It is obvious from Table 3 that the fluctuations of $\varepsilon_{Nd}(0)$ values in both of the Lingtai and Jinchuan profiles are

Table 3
The comparison between the data of Sun (2005) and us

	$^{143}Nd/^{144}Nd$ (average)	$\varepsilon_{Nd}(0)$	Difference
Sun (2005) (Jinchuan)			
Loess–paleosol (from 2.5 Ma B.P. to the present)	0.5120803	−10.8	
Red clay (from 8 Ma B.P. to 2.5 Ma B.P.)	0.5120973	−10.5	0.3
This study (Lingtai)			
Loess–paleosol (from 2.5 Ma B.P. to the present)		−9.3	
Red clay (from 7 Ma B.P. to 2.5 Ma B.P.)		−9.5	0.2

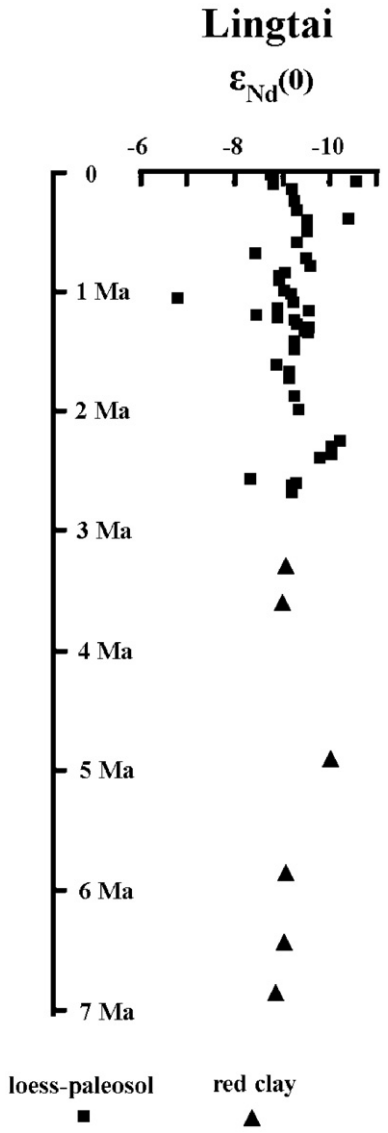

Fig. 2. Variations in $\varepsilon_{Nd}(0)$ of acid-insoluble residues from the Lingtai profile from 7 Ma B.P. to the present.

much smaller than 0.7ε units, i.e. the fluctuations are within the range of the experimental error.

Fig. 2 shows that there are four short positive fluctuations of $\varepsilon_{Nd}(0)$ in the Lingtai profile from 2.6 Ma B.P. to the present (~2.6 Ma B.P., $\varepsilon_{Nd}(0)=-8.3$; ~1.2 Ma B.P., $\varepsilon_{Nd}(0)=-8.4$; ~1.0 Ma B.P., $\varepsilon_{Nd}(0)=-6.9$; ~0.7 Ma B.P., $\varepsilon_{Nd}(0)=-8.3$). Three anomalous events since 2.6 Ma B.P. that took place at ~2.6 Ma B.P., 1.0 Ma B.P. and 0.7 Ma B.P., respectively, have been reported and might have been caused by impacts of extraterrestrial objects (e.g. Kyte and Browalee, 1985; Kyte et al., 1988; Margolis et al., 1991; Glass and Wu, 1993; Schmid et al., 1993). Another possibility may be the supply of young volcanic components with higher $\varepsilon_{Nd}(0)$ admixed to the Asian dust due to the large-scale volcanisms during the periods of the events (e.g., Asahara et al., 1999; Pettke et al., 2000). Furthermore, Prueher and Rea (2001) have provided a reliable investigation for the event at ~2.6 Ma B.P., which demonstrated that the mass accumulation rates of both glass and ice-rafted debris of North Pacific deep-sea sediment increased markedly at 2.65 Ma B.P. and the flux of the volcanic glass increased just prior to the flux of ice-rafted material, suggesting that the cooling resulting from explosive volcanic eruptions was the ultimate trigger for the intensification of Northern Hemisphere glaciation at approximately 2.6 Ma B.P. Therefore, the fluctuations in Nd isotopes towards higher values at ~2.6 Ma B.P. and ~1.0 Ma B.P. in the Loess Plateau of China revealed in the present study, seem likely to be corresponded with pulses of circum-Pacific explosive volcanism.

Controversies also exist about the origin of the red clay of the Loess Plateau. Some workers, mainly based on field observations or magnetic susceptibility anisotropy determinations, suggested that, similar to the overlying loess and paleosols, the red clay is of Eolian origin (Liu et al., 1988a; Evans et al., 1991; Ding et al., 1997; Sun et al., 1998). For example, Ding et al. (1998b, 1999) proposed that all of the red levels are of Eolian origin because they have similar grain-size distribution and REE patterns to the overlying loess–paleosols. However, Mo and Derbyshire (1991) believed that the red clay in the Jing–Le Basin was developed under warm/temperate and sub-humid conditions as a weathered mantle transported down gentle slopes by creep and rain wash. Evans et al. (1991) suggested that the upper part of the Red Clay Formation at Baoji might be of Eolian origin while the lower part may be of lacustrine origin. Rea et al. (1998) inferred that the upper sequence (<3.6 Ma B.P.) of the Red Clay Formation was of Eolian origin, while the older portion is water-lain. Guo et al. (2001) put forward that the lower part of the Red Clay Formation (>6.2 Ma B.P.) may be a water-reworked deposit related to alluvial and slope processes; the middle part (from ~6.2 to 3.6 Ma B.P.) was derived from in situ Eolian dust deposition; and the upper part (from ~3.6 to 2.6 Ma B.P.) is an Eolian dust deposition also.

The present study provides six $\varepsilon_{Nd}(0)$ values in the Red Clay Formation, two from the lower member of the Red Clay Formation, two from the middle member and two from the upper member. Our results exhibit a relatively narrow range from to −8.8 to −10.1, with an average of −9.5. The difference between the average

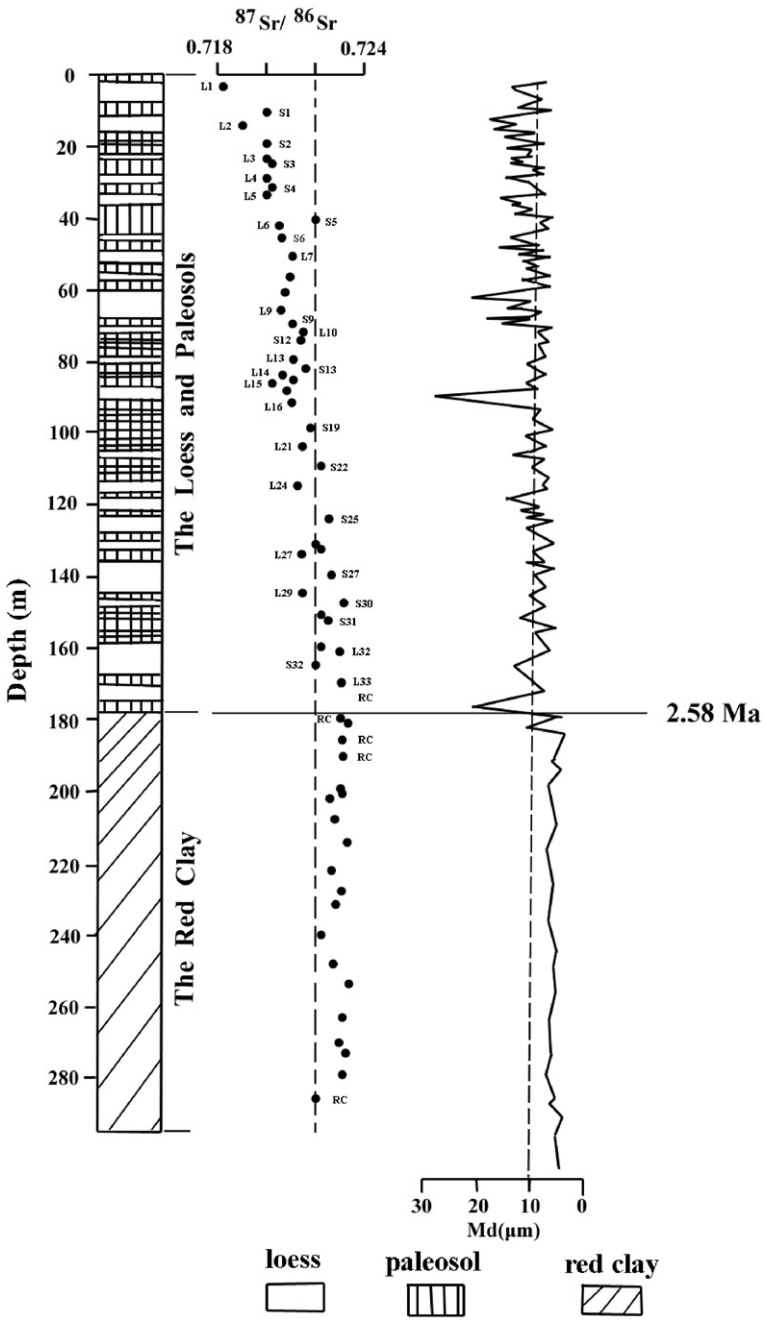

Fig. 3. Variations in $^{87}Sr/^{86}Sr$ ratios of acid-insoluble residues and median grain size (Md) (Ding et al., 2001a,b) from the Lingtai profile with sampling depth.

$\varepsilon_{Nd}(0)$ of the red clay and the overlying loess–paleosols is only 0.2ε units. Therefore, no matter how the red clay was deposited, the lower, middle and upper members of the Red Clay Formation have the identical source regions and the source regions of the red clay are the same as those of the overlying loess–paleosols.

4.2. Variations in $^{87}Sr/^{86}Sr$ in the Lingtai profile since 2.5 Ma B.P.

The variations of $^{87}Sr/^{86}Sr$ ratios of acid-insoluble residues from the Lingtai profile since 2.5 Ma B.P. are shown in Fig. 3. They have two features: (1) the

$^{87}Sr/^{86}Sr$ ratios of acid-insoluble residues in the loess levels are generally lower than those in the intercalated paleosol levels, (2) an overall descending trend is from 0.7230 at ~2.5 Ma B.P. to 0.7182 at the present.

In general, there are three possible interpretations for the variations of $^{87}Sr/^{86}Sr$ ratios of acid-insoluble residues of the whole Lingtai profile: provenance change, chemical weathering change, and grain-size distribution change.

As mentioned above, very few investigations on provenance change of the loess have been published until now. Gallet et al. (1996) and Jahn et al. (2001) investigated Nd and Sr isotopes using bulk soil samples of the Loess Plateau over the past 0.80 Ma to 0.14 Ma, respectively. Gallet et al. (1996) obtained nearly identical $\varepsilon_{Nd}(0)$ values for the bulk loess and paleosol samples in the Luochuan profile, which are in a range from −9.1 to −10.4 since 0.80 Ma B.P., with an average of −9.7. They concluded that Nd and Sr isotopic compositions of loess–paleosols are rather uniform and suggested a uniform source region during the period of loess deposition since 0.80 Ma B.P. No any other reliable evidence about provenance change has been reported until now, except that Sun (2005) considered that the source of the red clay sequence might be different from the overlying loess–paleosols. However, his inference might be problematic as we have pointed out above, based on his data and experimental error analysis. In the present study, our Nd isotopic data verify that the source areas of the loess of the Loess Plateau were generally stable since 7 Ma B.P.

The second interpretation is involved with chemical weathering. In essence, Sr (in particular the radiogenic fraction) in minerals is comparably soluble. Hence, enhanced rainfall may lead to enhanced chemical weathering, which in turn will preferentially remove the radiogenic portion of the host material, forming the basis for the leachate isotope approach. In this process, the Sr isotope ratio of the host material would be reduced as well. In the case of the Loess Plateau, the decrease in Sr isotopic composition in acid-insoluble residues of the Lingtai profile since 2.5 Ma B.P. would indicate a long-term increase in chemical weathering. But this interpretation of chemical weathering is in a strong contradiction with the fact that the $^{87}Sr/^{86}Sr$ ratios of acid-insoluble residues in the loess are usually lower than those in the intercalated paleosol levels. It is generally accepted now that the loess of the Loess Plateau accumulated by higher atmospheric dust influx under a strong winter monsoon (weak chemical weathering) during glacial periods, while the paleosol was developed under an intensified summer monsoon (strong chemical weathering) and a weakened winter monsoon during interglacial periods (Liu, 1985; Kukla and An, 1989; An et al., 1991a; Rutter and Ding, 1993).

The third interpretation is related to grain-size distribution change. Dasch (1969) and Biscaye and Dasch (1971) have argued that Sr isotopic ratios of the loess could be a function of grain sizes, depending on monsoon intensity during Eolian transport, and therefore provided less information about provenance than desired. In order to further verify the influence of grain sizes on the Sr isotopic ratio, we selected three samples (one loess, one paleosol and one red clay) and separated them into four grain-size fractions, and the Sr isotopic composition of acid-insoluble residue of each fraction was analyzed. The sorting method of grain-size fractions was the same as described above. The Sr isotope results are shown in Table 4. Clearly, all of the fine grain-size fractions (<2 μm) have higher $^{87}Sr/^{86}Sr$ ratios than the bulk soil samples and coarser grain-size fractions.

One of the consequences of the intense winter monsoon is grain-size sorting during Eolian transport, meantime leading to mineral sorting as well. The ratio of fine to coarse grain-size fractions in the loess of the Loess Plateau decreased during the strong winter monsoon; however, the ratio of fine to coarse grain-size fractions in paleosols increased during the weak winter monsoon. Therefore, the $^{87}Sr/^{86}Sr$ ratio of acid-insoluble residue of the loess is a proxy indicator of the winter monsoon, and the curve of $^{87}Sr/^{86}Sr$ ratios of acid-insoluble residues of the Lingtai profile may reflect variations in the winter monsoon intensity since 7.0 Ma B.P.

Previous studies on mineralogy of the loess and paleosols of the Loess Plateau have revealed that they consist mostly of quartz, mica, feldspar, carbonate and clay minerals, and that these clay minerals are finer

Table 4
The $^{87}Sr/^{86}Sr$ ratios of acid-insoluble residues of four grain-size fractions for the selected three samples (one loess, one paleosol and one red clay) from the Lingtai profile

Sample depth (m)	Bulk soil sample	>45 μm sample	45–28 μm sample	28–2 μm sample	<2 μm sample
71.30 (L)	0.720951 (10)	0.722665 (18)	0.719476 (7)	0.720302 (10)	0.726261 (9)
165.40 (S)	0.720509 (12)	0.718122 (20)	0.720316 (18)	0.719415 (13)	0.729943 (29)
273.40 (RC)	0.721554 (18)	0.719930 (13)	0.720479 (28)	0.719946 (12)	0.725733 (9)

$^{87}Sr/^{86}Sr$ normalized to $^{86}Sr/^{88}Sr=0.1194$. The numbers in brackets represent error (2σm). RC—red clay, L—loess, S—paleosol.

grained than the silt-sized quartz and feldspar grains and are concentrated in the <2 μm grain-size fraction (Liu, 1985; Zheng et al., 1994). As mentioned above, the loess of the Loess Plateau was formed under a strong winter monsoon during glacial periods, while the paleosols were developed under an intensified summer monsoon and weak winter monsoon in interglacial and interstadial periods. This gave rise to more clay minerals (with high Rb/Sr and $^{87}Sr/^{86}Sr$ ratios) and less feldspars in the paleosols than in the loess, leading to the paleosol with higher $^{87}Sr/^{86}Sr$ ratios than the loess.

The variations in $^{87}Sr/^{86}Sr$ ratios of acid-insoluble residues of the Lingtai profile in Fig. 3 can be divided into two stages. The first stage is the Red Clay Formation from ~7 Ma B.P. to 2.5 Ma B.P. and is characterized by a high average ratio of 0.7230. The second stage is the overlying loess–paleosols and the $^{87}Sr/^{86}Sr$ ratios display an overall descending trend from 0.7230 at ~2.5 Ma B.P. to 0.7182 at the present. This result implies that the East Asian winter monsoon was weak and relatively stable from ~7 Ma B.P. to ~2.5 Ma B.P. and that it was continuously enhanced from ~2.5 Ma B.P. to the present.

Median grain size (Md) (the fiftieth percentile value of the grain-size distribution). is lower in the paleosols than the loess (Zheng et al., 1994; Lu and An, 1997). The concentration of coarse grain-size or median grain-size (Md) fractions has been used as a proxy indicator of the winter monsoon intensity (Lu and An, 1997; An et al., 2001).

Fig. 3 shows that Md in the Lingtai profile is generally low in the first stage from ~7 Ma B.P. to 2.5 Ma B.P., but shows a higher variability and a gradually increasing trend at the second stage from ~2.5 Ma B.P. to the present. The Md variation is similar to that of $^{87}Sr/^{86}Sr$ ratios of acid-insoluble residues in the Lingtai profile. The fluctuations of both $^{87}Sr/^{86}Sr$ ratios and Md of the Lingtai profile imply: (1) the East Asian winter monsoon might be weak from ~7 Ma B.P. to ~2.5 Ma B.P., (2) the East Asian winter monsoon strengthened from ~2.5 Ma B.P. to the present, and (3) ~2.5 Ma B.P. was a pivot between these two stages. These conclusions are consistent with the climate-model simulations for glacial conditions (Prell and Kutzbach, 1992). The major Northern Hemisphere glaciation began at ~2.5 Ma B.P. and the strengthened winter monsoon northwesterly winds across eastern Asian. Continued aridity in central Asian were caused by the Quaternary climatic fluctuations on the glacial–interglacial timescale, which may be genetically related to continued uplift and expansion of the Tibet–Qinghai Plateau along its northern and eastern margins (An et al., 2001).

On the basis of the temporal variations of the monsoon indices, mainly magnetic susceptibility and coarse grain-size fraction, Rb/Sr ratio and Eolian flux, An et al. (2001) divided the East Asian climate from 6 to 2 Ma B.P. into three intervals. The period from 6 to ~3.6 Ma B.P. was characterized by considerable variability of the monsoon indices but relatively small trends. The period from about 3.6 to 2.5 Ma B.P. contained simultaneous intensification of both summer and winter monsoon on the Loess Plateau, as well as a sustained increase of Eolian flux to the North Pacific. After 2.5 Ma B.P., the East Asian summer monsoon becomes more variable and the East Asian winter monsoon intensified. The investigation of Rea et al. (1998) also clearly showed that an increase in Asian dust flux to the Pacific occurred at 3.6 Ma B.P. The present investigation of $^{87}Sr/^{86}Sr$ ratios of the Lingtai profile has obtained similar results to those of An et al. (2001) at two intervals from 6 to ~3.6 Ma B.P. and from 2.5 Ma B.P. to the present, but the change of another interval from ~3.6 to 2.5 Ma B.P. has not been observed. The Nd fluctuation of the Lingtai profile also is not compatible with such variations in the 3.6–2.5 Ma B.P. interval (Fig. 3).

5. Conclusions

The following conclusions can be drawn by the present study on Nd and Sr isotopes of acid-insoluble residues from the Lingtai profile of the Loess Plateau:

(1) $^{87}Sr/^{86}Sr$ ratios of acid-insoluble residues in the loess levels are generally lower than those in the intercalated paleosol levels. It is attributed to finer grain-size fractions or more clay minerals in the paleosol than in the loess.

(2) Variations in $^{87}Sr/^{86}Sr$ ratios can be divided into two stages. The first stage (~7 Ma B.P. to 2.5 Ma B.P.) is characterized by an average value of 0.7230. In the second stage the $^{87}Sr/^{86}Sr$ ratios display a stronger variability and overall descending trend from 0.7230 at ~2.5 Ma B.P. to 0.7182 at the present. This stage includes the Wuchen Loess (WL4-WS1), the Lishi Loess (L15-S1), the Malan Loess (L1) and the Holocene Loess (S0). It implies that the East Asian winter monsoon was weak and relatively stable from ~7 Ma B.P. to ~2.5 Ma B.P. and that it was continuously enhanced from ~2.5 Ma B.P. to the present.

(3) Based on Nd isotopes, the source areas of the Loess Plateau may have been relatively constant since 7 Ma B.P., and both red clay and overlying loess–paleosols may have the same source regions.

Acknowledgements

This research was supported by the National Natural Science Foundation of China (grants 40473009 and

40331001). We are grateful to Z.S. An and Y.B. Sun for providing the samples of the Lingtai profile, and to two anonymous reviewers for their constructive and thoughtful review comments, which significantly improved the manuscript.

References

An, Z.S., Kukla, G.J., Porter, S.C., Xiao, J.L., 1991a. Magnetic susceptibility evidence of monsoon variation on the Loess Plateau of Central China during the last 130,000 years. Quat. Res. 36, 29–36.

An, Z.S., Kukla, G.J., Porter, S.C., 1991b. Late Quaternary dust flow on the Chinese Loess Plateau. Catena 18, 125–132.

An, Z.S., Kutzbach, J.E., Prell, W.L., Porter, S.C., 2001. Evolution of Asian monsoon and phased uplift of the Himalaya–Tibetan plateau since Late Miocene times. Nature 411, 62–66.

Asahara, Y., Tanaka, T., Kamioka, H., Nishimura, A., 1995. Asian continental nature of $^{87}Sr/^{86}Sr$ ratios in north central Pacific sediments. Earth Planet. Sci. Lett. 133, 105–116.

Asahara, Y., Tanaka, T., Kamioka, H., Nishimura, A., Yamazaki, T., 1999. Provenance of the north Pacific sediments and process of source material transport as derived from Rb–Sr isotopic systematics. Chem. Geol. 158, 271–291.

Biscaye, P.E., Dasch, E.J., 1971. The rubidium, strontium and strontium isotope system in deep-sea sediments: Argentine Basin. J. Geophys. Res. 76, 5087–5096.

Biscaye, P.E., Grousset, F.E., Revel, M., Van der Gaast, S., Zielinski, G.A., Vaars, A., Kukla, G., 1997. Asian provenance of glacial dust (stage 2) in the Greenland Ice Sheet Project 2 ice core, Summit, Greenland. J. Geophys. Res. 102, 26765–26781.

Bory, A.J.-M., Biscaye, P.E., Grousset, F.E., 2003. Two distinct seasonal Asian source regions for mineral dust deposited in Greenland (North GRIP). Geophys. Res. Lett. 30, 16-1–16-4.

Chang, Q., Mishima, T., Yabuki, S., Takahashi, Y., Shimitu, H., 2000. Sr and Nd isotope ratios and REE abundances of moraines in the mountain areas surrounding the Taklimakan Desert, NW China. Geochem. J. 34, 407–427.

Chen, J., Qiu, G., Yang, J.D., 1997. Sr isotopic composition of loess carbonate and identification of primary and secondary carbonates. Prog. Nat. Sci. 7, 590–593.

Chen, J., Wang, Y.J., Chen, Y., Liu, L.W., Ji, J.F., Lu, H.Y., 2000. Rb and Sr geochemical characterization of the Chinese Loess stratigraphy and its implications for palaeomonsoon climate. Acta Geol. Sin. 74, 279–288.

Dasch, E.J., 1969. Strontium isotopes in weathering profile, deep sea sediments and sedimentary rocks. Geochim. Cosmochim. Acta 33, 1521–1552.

Ding, Z.L., Rutter, N.W., Han, J.T., Liu, T.S., 1992. A coupled environmental system formed at about 2.5 Ma over Eastern Asia. Palaeogeogr. Palaeoclimatol. Palaeoecol. 94, 223–242.

Ding, Z.L., Rutter, N.W., Liu, T.S., 1993. Pedostratigraphy of Chinese Loess deposits and climatic cycles in the last 2.5 Ma. Catena 20, 73–91.

Ding, Z.L., Rutter, N.W., Liu, T.S., 1997. The onset of extensive loess deposition around the G/M boundary in China and its palaeoclimatic implications. Quat. Int. 40, 53–60.

Ding, Z.L., Sun, J.M., Liu, T.S., Zhu, R.X., Yang, S.L., Guo, B., 1998a. Wind-blown origin of the Pliocene Red Clay Formation in the central Loess Plateau, China. Earth Planet. Sci. Lett. 161, 135–143.

Ding, Z.L., Sun, J.M., Yang, S.L., Liu, T.S., 1998b. Preliminary magnetostratigraphy of a thick Eolian red clay–loess sequence at Lingtai, the Chinese Loess Plateau. Geophys. Res. Lett. 25, 1225–1228.

Ding, Z.L., Xiong, S.F., Sun, J.M., Yang, S.L., Gu, Z.Y., Liu, T.S., 1999. Pedostratigraphy and paleomagnetism of a ~7.0 Ma Eolian loess–red clay sequence at Lingtai, Loess Plateau, north-central China and the implications for paleomagnetism evolution. Palaeogeogr. Palaeoclimatol. Palaeoecol. 152, 49–66.

Ding, Z.L., Rutter, N.W., Sun, J.M., Yang, S.L., Liu, T.S., 2000. Rearrangement of atmospheric circulation at about 2.6 Ma over northern China: evidence from grain size records of loess–paleosol and red clay sequences. Quat. Sci. Rev. 19, 547–558.

Ding, Z.L., Yang, S.L., Sun, J.M., Liu, T.S., 2001a. Iron geochemistry of loess and red clay deposits in the Chinese Loess Plateau and implications for long-term Asian monsoon evolution in the last 7.0 Ma. Earth Planet. Sci. Lett. 185, 99–109.

Ding, Z.L., Sun, J.M., Yang, S.L., Liu, T.S., 2001b. Geochemistry of the Pliocene Red Clay Formation in the Chinese Loess Plateau and implications for its origin, source provenance and paleoclimate change. Geochim. Cosmochim. Acta 65, 901–913.

Evans, M.E., Wang, Y., Rutter, N., Ding, Z.L., 1991. Preliminary magnetostratigraphy of the red clay underlying the loess sequence at Baoji, China. Geophys. Res. Lett. 18, 1409–1412.

Gallet, S., Jahn, B.M., Torii, M., 1996. Geochemical characterization of the Luochuan loess–paleosol sequence, China, and paleoclimate implications. Chem. Geol. 133, 67–88.

Glass, B.P., Wu, J., 1993. Coesite and shocked quartz discovered in the Australasian and North American microtektite layers. Geology 21, 435–438.

Goldstein, S.L., Jacobsen, S.B., 1988. Nd and Sr isotopic systematics of river water suspended material: Implications for crustal evolution. Earth Planet. Sci. Lett. 87, 249–265.

Golstein, S.L., O'Nions, R.K., Hamilton, P.J., 1984. A Sm–Nd isotopic study of atmospheric dusts and particulates from major river systems. Earth Planet. Sci. Lett. 70, 221–236.

Grousset, F.E., Biscaye, P.E., 2005. Tracing dust source and transport patterns using Sr, Nd and Pb isotopes. Chem. Geol. 222, 149–167.

Guo, Z.T., Peng, S.Z., Hao, Q.Z., Biscaye, P.E., Liu, T.S., 2001. Origin of the Miocene–Pliocene Red Earth Formation at Xifeng in northern China and implications for paleoenvironments. Palaeogeogr. Palaeoclimatol. Palaeoecol. 170, 11–26.

Guo, Z.T., Peng, S.Z., Hao, Q.Z., Biscaye, P.E., An, Z.S., Liu, T.S., 2004. Late Miocene–Pliocene development of Asian aridification as recorded in the Red-Earth Formation in northern China. Glob. Planet. Change 41, 135–145.

Heller, F., Liu, T.S., 1982. Magnetostratigraphic dating of loess deposits in China. Nature 300, 431–433.

Heller, F., Shen, C., Beer, J., Liu, X.M., Liu, T.S., 1993. Quantitative estimates of pedogenic ferromagnetic mineral formation in Chinese Loess and paleoclimatic implications. Earth Planet. Sci. Lett. 114, 385–390.

Honda, M., Shimizu, H., 1998. Geochemical, mineralogical and sedimentological studies on the Taklimakan Desert sands. Sedimentology 45, 1125–1143.

Jahn, B.M., Gallet, S., Han, J., 2001. Geochemistry of the Xining, Xifeng and Jixian sections, Loess Plateau of China: Eolian dust provenance and paleosol evolution during the last 140 ka. Chem. Geol. 178, 71–94.

Jones, C.E., Halliday, A.N., Rea, D.K., Owen, R.M., 1994. Neodymium isotopic variations in North Pacific modern silicate sediment and the insignificance of detrital REE concentrations to seawater. Earth Planet. Sci. Lett. 127, 55–66.

Kanayama, S., Yabuki, S., Yanagisawa, F., Motoyama, R., 2002. The chemical and strontium isotope composition of atmospheric aerosols over Japan: the contribution of long-range-transported Asian dust (Kosa). Atmos. Environ. 36, 5159–5175.

Kukla, G., An, Z.S., 1989. Loess stratigraphy in central China. Palaeogeogr. Palaeoclimatol. Palaeoecol. 72, 203–225.

Kyte, F.T., Browalee, D.E., 1985. Unmelted meteoritic debris in the late Pliocene iridium anomaly: evidence for the ocean impact of a non-chondritic asteroid. Geochim. Cosmochim. Acta 49, 1095–1108.

Kyte, F.T., Zhou, L., Wasson, J.T., 1988. New evidence on the size and possible effects of a late Pliocene oceanic asteroid impact. Science 241, 63–65.

Liu, T.S., 1985. Loess and the Environment. China Ocean Press, Bejing. (in Chinese).

Liu, C.Q., Masuda, A., Okada, A., Yabuki, S., Fan, Z.L., 1994. Isotope geochemistry of Quaternary deposits from the arid lands in northern China. Earth Planet. Sci. Lett. 127, 25–38.

Liu, X.M., Rolph, T., Bloemendal, J., Shaw, J., Liu, T.S., 1995. Quantitative estimates of palaeoprecipitation at Xifeng area, in the Loess Plateau of China. Palaeogeogr. Palaeoclimatol. Palaeoecol. 113, 243–248.

Liu, X.M., Liu, T.S., Xu, T.C., Liu, C., Chen, M.Y., 1988a. The Chinese Loess in Xifeng, I. The primary study on magnetostratiography of a loess profile in Xifeng area, Gansu province. Geophys. J. 92, 345–348.

Liu, X.M., Xu, T.C., Liu, T.S., 1988b. The Chinese Loess in Xifeng, II. A study of anisotropy of magnetic susceptibility of loess from Xifeng. Geophys. J. 92, 349–353.

Lu, H.Y., An, Z.S., 1997. Paleoclimatic significance of grain-size distribution of the Luochuan Loess. Chin. Sci. Bull. 42, 66–69 (in Chinese).

Maher, B.A., Thompson, R., Zhou, L.P., 1994. Spatial and temporal reconstructions of changes in the Asian palaeomonsoon: a new mineral magnetic approach. Earth Planet. Sci. Lett. 125, 462–471.

Margolis, S.V., Clseys, P., Kyte, F.T., 1991. Microtektites, microkrystites, and spinels from a late Pliocene asteroid impact in the Southern Ocean. Science 251, 1594–1596.

Mo, D.W., Derbyshire, E., 1991. The depositional environment of the late Pliocene red clay, Jing–Le Basin, Shanxi province, China. Sediment. Geol. 70, 33–40.

Nakai, S.N., Halliday, A.N., Rea, D.K., 1993. Provenance of dust in the Pacific Ocean. Earth Planet. Sci. Lett. 119, 143–157.

Nakano, T., Yokoo, Y., Nishikawa, M., Koyanagi, H., 2004. Regional Sr–Nd isotopic ratios of soil minerals in northern China as Asian dust fingerprints. Atmos. Environ. 38, 3061–3067.

Pettke, T., Halliday, A.N., Hall, C.M., Rea, D.K., 2000. Dust production and deposition in Asia and the north Pacific Ocean over the past 12 Myr. Earth Planet. Sci. Lett. 178, 397–413.

Porter, S.C., An, Z.S., 1995. Correlation between climate events in the North Atlantic and China during the last glaciation. Nature 375, 305–308.

Prell, W.L., Kutzbach, J.E., 1992. Sensitivity of the Indian monsoon to forcing parameters and implications for its evolution. Nature 360, 647–652.

Prueher, L.M., Rea, D.K., 2001. Volcanic triggering of late Pliocene glaciation: evidence from the flux of volcanic glass and ice-rafted debris to the North Pacific Ocean. Palaeogeogr. Palaeoclimatol. Palaeoecol. 173, 215–230.

Rea, D.K., Snoeckx, H., Joseph, L.H., 1998. Late Cenozoic Eolian deposition in the North Pacific: Asian drying, Tibetan uplift, and cooling of the Northern Hemisphere. Paleoceanography 13, 215–224.

Revel, M., Sinko, J.A., Grousset, F.E., 1996. Sr and Nd isotopes as tracers of North Atlantic lithic particles: paleoclimatic implications. Paleoceanography 11, 95–113.

Rousseau, D.D., Wu, N.Q., 1997. A new molluscan record of the monsoon variability over the past 130000 yr in the Luochuan Loess sequence, China. Geology 25, 275–278.

Rutter, N.W., Ding, Z.L., 1993. Palaeoclimates and monsoon variations interpreted from microporphogenic features of the Baoji palaeosols, China. Quat. Sci. Rev. 12, 853–862.

Rutter, N.W., Ding, Z.L., Evans, M.E., Wang, Y.C., 1990. Magnetostratigraphy of the Baoji loess–paleosol section in the north-central China Loess Plateau. Quat. Int. 7-8, 97–102.

Schmid, G., Zhou, L., Wasson, J.T., 1993. Iridium anomaly associated with the Australasian tektite-producing impact: masses of the impactor and of the Australasian tektites. Geochim. Cosmochim. Acta 57, 4851–4859.

Sheng, X.F., Yang, J.D., Li, C.L., Chen, J., Tao, X.C., 2000. The method experiments to separate calcite and dolomite from loess and sediments. Rock Miner. Anal. 19, 264–267 (in Chinese).

Sun, J.M., 2005. Nd and Sr isotopic variations in Chinese Eolian deposits during the past 8 Ma: implications for provenance change. Earth Planet. Sci. Lett. 240, 454–466.

Sun, Y.B., An, Z.S., 2002. History and variability of Asian interior aridity recorded by Eolian flux in the Chinese Loess Plateau during the past 7 Ma. Sci. China, Ser. D: Earth Sci. 45, 420–429.

Sun, X.J., Song, C.Q., Wang, F.Y., Sun, M.R., 1997. Vegetation history of the Loess Plateau of China during the last 100000 years based on pollen data. Quat. Int. 37, 25–36.

Sun, D.H., An, Z.S., Shaw, J., Bloemendal, J., Sun, Y.B., 1998. Magnetostratigraphy and paleoclimatic significance of late Tertiary Aeolian sequences in the Chinese Loess Plateau. Geophys. J. Int. 134, 207–212.

Xiao, J.L., Porter, S.C., An, Z.S., Kumai, H., Yoshikawa, S., 1995. Grain size of quarts as an indicator of winter monsoon strength on the Loess Plateau of central China during the last 130000 yr. Quat. Res. 43, 22–29.

Yang, J.D., Tao, X.C., Xue, Y.S., 1997. Nd isotopic variations of Chinese seawater during Neoproterozoic through Cambrian. Chem. Geol. 135, 127–137.

Yang, J.D., Chen, J., An, Z.S., Shields, G., Tao, X.C., Zhu, H.B., Ji, J.F., Chen, Y., 2000. Variations in $^{87}Sr/^{86}Sr$ ratios of calcites in Chinese Loess: a proxy for chemical weathering associated with the East Asian summer monsoon. Palaeogeogr. Palaeoclimatol. Palaeoecol. 157, 151–159.

Yang, J.D., Chen, J., Tao, X.C., Li, C.L., Ji, J.F., Chen, Y., 2001. Sr isotope ratios of the acid-leached loess residues from Luochuan, China: a tracer of continental weathering intensity over the past 2.5 Ma. Geochem. J. 35, 403–412.

Yokoo, Y., Nakano, T., Nishikawa, M., Quan, H., 2001. The importance of Sr isotopic compositions as an indicator of acid-soluble minerals in arid soils in China. Water Air Soil Pollut. 130, 763–768.

Yokoo, Y., Nakano, T., Nishikawa, M., Quan, H., 2004. Mineralogical variation of Sr–Nd isotopic and elemental compositions in loess and desert sand from the central Loess Plateau in China as a provenance tracer of wet and dry deposition in the northwestern Pacific. Chem. Geol. 204, 45–62.

Zheng, H.B., An, Z.S., Shaw, J., Liu, T.S., 1991. A detailed terrestrial geomagnetic record for the interval 0–5.0 Ma. In: Liu, T.S., Ding, Z.L., Guo, Z.T. (Eds.), Loess Environment and Global Change. Science Press, Beijing, pp. 147–156.

Zheng, H.H., Theng, B.K.G., Whitton, J.S., 1994. Mineral composition of loess–paleosol in the Loess Plateau of China and its environmental implications. Geochimica 23, 113–123.